LSTM Recurrent Neural Network Classifier for High Impedance Fault Detection in Solar PV Integrated Power System

Veerasamy, Veerapandiyan; Wahab, Noor Izzri Abdul; Othman, Mohammad Lutfi; Padmanaban, Sanjeevikumar; Sekar, Kavaskar; Ramachandran, Rajeswari; Hizam, Hashim; Vinayagam, Arangarajan; Islam, Mohammad Zohrul

Published in:
IEEE Access

DOI (link to publication from Publisher):
10.1109/ACCESS.2021.3060800

Publication date:
2021

Document Version
Publisher's PDF, also known as Version of record

IEEE Access
Multidisciplinary | Rapid Review | Open Access Journal

SPECIAL SECTION ON EVOLVING TECHNOLOGIES IN ENERGY STORAGE SYSTEMS FOR ENERGY SYSTEMS APPLICATIONS

Received February 5, 2021, accepted February 13, 2021, date of publication February 22, 2021, date of current version March 2, 2021.

Digital Object Identifier 10.1109/ACCESS.2021.3060800

LSTM Recurrent Neural Network Classifier for High Impedance Fault Detection in Solar PV Integrated Power System

VEERAPANDIYAN VEERASAMY[1], (Graduate Student Member, IEEE), NOOR IZZRI ABDUL WAHAB[1], (Senior Member, IEEE), MOHAMMAD LUTFI OTHMAN[1], (Senior Member, IEEE), SANJEEVIKUMAR PADMANABAN[2], (Senior Member, IEEE), KAVASKAR SEKAR[3], RAJESWARI RAMACHANDRAN[4], (Member, IEEE), HASHIM HIZAM[1], (Member, IEEE), ARANGARAJAN VINAYAGAM[5], (Member, IEEE), AND MOHAMMAD ZOHRUL ISLAM[1], (Graduate Student Member, IEEE)

[1]Advanced Lightning Power and Energy Research (ALPER), Department of Electrical and Electronics Engineering, Universiti Putra Malaysia (UPM), Seri Kembangan 43400, Malaysia
[2]Department of Energy Technology, Aalborg University Esbjerg, 6700 Esbjerg, Denmark
[3]Department of Electrical and Electronics Engineering, Panimalar Engineering College, Chennai 600123, India
[4]Department of Electrical and Electronics Engineering, Government College of Technology, Coimbatore 641013, India
[5]Department of Electrical and Electronics Engineering, New Horizon College of Engineering, Bengaluru 560103, India

Corresponding authors: Veerapandiyan Veerasamy (veerapandian220@gmail.com) and Noor Izzri Abdul Wahab (izzri@upm.edu.my)

This work was supported by the Geran Putra Berimpak -University Putra Malaysia (GPB-UPM), Malaysia, under Grant 9671700.

ABSTRACT This paper presents the detection of High Impedance Fault (HIF) in solar Photovoltaic (PV) integrated power system using recurrent neural network-based Long Short-Term Memory (LSTM) approach. For study this, an IEEE 13-bus system was modeled in MATLAB/Simulink environment to integrate 300 kW solar PV systems for analysis. Initially, the three-phase current signal during non-faulty (regular operation, capacitor switching, load switching, transformer inrush current) and faulty (HIF, symmetrical and unsymmetrical fault) conditions were used for extraction of features. The signal processing technique of Discrete Wavelet Transform with db4 mother wavelet was applied to extract each phase's energy value features for training and testing the classifiers. The proposed LSTM classifier gives the overall classification accuracy of 91.21% with a success rate of 92.42 % in identifying HIF in PV integrated power network. The prediction results obtained from the proffered method are compared with other well-known classifiers of K-Nearest neighbor's network, Support vector machine, J48 based decision tree, and Naïve Bayes approach. Further, the classifier's robustness is validated by evaluating the performance indices (PI) of kappa statistic, precision, recall, and F-measure. The results obtained reveal that the proposed LSTM network significantly outperforms all PI compared to other techniques.

INDEX TERMS Solar photovoltaic, high impedance fault, discrete wavelet transform, recurrent neural network, long-short term memory.

ABBREVIATIONS

RE	Renewable Energy
MG	Microgrid
PVDG	Photovoltaic Distributed Generation
HIF	High Impedance Fault
PV	Photovoltaic
RNN	Recurrent Neural Network
LSTM	Long Short Term Memory
JDT	J48 Decision Tree
WT	Wavelet Transform
ANFIS	Adaptive Neuro-Fuzzy Inference System
CNN	Convolutional Neural Network
PMU	Phasor Measurement Unit
MODWPT	Maximum Overlap Discrete Wavelet Packet Transform

The associate editor coordinating the review of this manuscript and approving it for publication was Giambattista Gruosso.

DFT	Discrete Fourier Transform
KF	Kalman Filter
DT	Decision Tree
DWT	Discrete Wavelet Transform
SVM	Support Vector Machine
KNN	K-Nearest Neighbors Network
Db4	Daubechies 4 mother wavelet
PIs	Performance Indices
SPT	Signal Processing Techniques
FFT	Fast Fourier Transform
LLG	Double Line to Ground fault
LLLG	Three-phase fault
DC	Direct Current
AC	Alternating Current
VSI	Voltage Source Inverter
MPPT	Maximum Power Point Tracking
IGBT	Insulated-gate Bipolar Transistor
PWM	Pulse Width Modulation
THD	Total Harmonic Distortion
NB	Naïve Bayes
IEEE	Institute of Electrical and Electronics Engineers
I-V	Current-Voltage characteristics
P-V	Power-Voltage characteristics
STC	Standard Test Conditions of Solar PV with temperature (T = 25°C) and irradiance of 1000 W/m^2
LG	Single Line to Ground fault
LL	Double Line Fault
CA	Classification Accuracy
CWT	Continuous Wavelet Transform
EV	Energy Value
ANN	Artificial Neural Network
RBF	Radial Basis Function
LIBSVM	A Library for SVM
KS	Kappa Statistics
P,R	Precision, Recall

I. INTRODUCTION

The ever-increasing load demand and a considerable decline in fossil fuels over the last few decades pave the way for adopting alternative energy sources to meet the energy requirement. The effectiveness of distributed energy sources involving RE or conventional synchronous generators into distribution network for providing high-quality power led to MG's concept. In the present energy scenario, the solar PVDG has been widely adopted in many countries compared to other RE sources due to its abundance in nature, lower weight, and economic feasibility [1]. Because of this, MG's secure and reliable operation is more important by designing a proper protection scheme that can detect, classify, and locate the system's fault. However, the conventional protection relay effortlessly can identify the low-impedance fault that occurs in the network. But, the HIF was unidentified because of its low magnitude of fault current. This induces a severe threat to public safety.

Moreover, the escalation of HIF into a healthy part of the grid system results in cascading failure of the power network [2], [3]. Therefore, detection of HIF is more critical in RE integrated distribution system. Also, most of the literature on the detection of fault was studied on a conventional system without considering RE sources. However, the present work focuses on detecting HIF in solar PV power networks using an RNN-based LSTM network. The detection of HIF involves a two-stage process: feature extraction and classifier construction [4].

Many SPT were proposed in the literature to extract features to train and test the classifiers in the pattern recognition stage. This process distinguishes the various disturbances by obtaining appropriate patterns using time-frequency transforms [5]. The FFT possesses spectral leakage and loss of time information on analyzing the signal for feature extraction. The STFT was widely used for fault analysis. However, it is also unsuitable because of its fixed window length for analyzing the non-stationary transient signals that comprise both time and frequency components [6].To resolve this, WT based techniques have been widely used for analyzing the transient signals that are non-periodic, which comprises impulse and sinusoidal component [7]. The WT generally exists in the continuous and discrete form; the latter was extensively used in power system applications like power quality and fault analysis. The DWT offers the advantages of adaptive window size with a pre-defined filter design [8]. Therefore, DWT has been used in the pre-processing stage of the classifier compared to other SPTs. Hence, the energy value feature was extracted from each phase's current signal using DWT analysis to train and test the proposed LSTM classifier to identify the HIF in the PV power network.

Various intelligence classifier approaches with SPTs were adopted for identifying the HIF in the power system. The literature studied in [9]–[15], applied a DWT analysis with multi-layer perceptron neural network, Fuzzy approach, ANFIS, SVM, Elman neural network to detect and classify the HIF in power distribution network. In [16], a WT and CNN were used for identifying the HIF in distribution network with real-time data acquisition using PMU. The MODWPT has been employed for detection of HIF in 13-bus distribution network with non-linear load to prove its adaptability in [17]. However, this study gives a HIF detection accuracy of 85.86%. On the flip-side, a combination of DFT and KF was used to detect the HIF and other conventional symmetrical and unsymmetrical faults in distribution network. The feature extracted is used to frame the digital logic to detect the faults in the system which gives the accuracy of 97 % [18]. However, this method is complex for large-scale system due to the multiple logics presented to detect the HIF. The authors in [19], presents a DWT based CNN for detection of HIF by combining the features from various distribution networks through the cloud-edge-collaboration framework with the development of internet of things. In [20], a modified

FFT based technique was used to identify the occurrence of HIF in IEEE 13-bus distribution network considering the non-linear loads and switching transients. A combination of variational mode decomposition and Teager-Kaiser energy operators were used to discriminate HIF from other transient phenomenon (load and capacitor switching) and normal conditions [21]. However, the study cannot consider the conventional symmetrical and unsymmetrical faults besides HIF. A mathematical morphology was used for identification of HIF in low voltage DC distribution network [22]. The study in [23], presents a Hibert-Huang Transform and machine learning techniques for detection of HIF and conventional faults in MG. This study reveals that the extreme learning machine gives an accuracy of 93 % and also outperforms than SVM and NB classifier. However, superior performance was seen using NB classifier for identification of symmetrical and unsymmetrical faults in a series compensated transmission system [24].The authors in [25], studied the detection of HIF using mathematical morphology during high penetration of solar photovoltaic (PV) in distribution network. However, the study does not consider the impact of conventional faults and switching events. But, this paper considers the identification of HIF in PV integrated distribution network by considering the switching events (capacitor and load switching), transformer inrush current, symmetrical and unsymmetrical faults. Even though, many techniques were presented for identification of HIF using various SPT and machine learning methods. The DWT based SPT was widely used in the pre-processing stage of classification model for the decomposition of signal into high and low frequency band in both time and frequency domain.

The evolution of the deep learning method for processing sequential data plays a vital role in applications like solar PV fault identification, electricity price prediction, short-term wind power forecasting, and so on [26]–[29]. Long Short-Term Memory is a unique recurrent neural network and powerful deep learning technique. This method differs from traditional neural networks because the neurons have a connection in forward as well as backward either to the same or previous layers. The LSTM can also better capture the features and handle data with irregularities than other machine learning techniques. This characteristic helps to detect the intermittent, asymmetry, random behavior possessed by the HIF current waveform, which the conventional protection scheme cannot detect. Thus, this paper proposes a DWT and LSTM based detection of HIF in PV integrated power network. The main contributions of this paper are:

- A deep learning method of RNN based LSTM network has been developed with feature extraction using DWT analysis to detect and classify the HIF in PV integrated power network.
- The extracted energy value features from DWT analysis of the current signal is used to train and test the proposed LSTM and other intelligent classifiers such as KNN, SVM, JDT, and NB. Then, the results obtained from various classifiers to detect HIF in PV power networks are compared.
- To validate the proposed classification model's performance, a comprehensive evaluation of classification accuracy, success rate, and other performance indices of Precision, Recall, F-Measure, and Kappa statistics were examined.

TABLE 1. Specification of PV panel.

Parameters	Specification
Temperature	25°C
Irradiance	1000 W/m^2
Maximum Power (P_{max})	305.266 W
The voltage at maximum power point (V_{mp})	54.7 V
Open Circuit Voltage (V_{oc})	64.2 V
Short circuit current (I_{sc})	5.96 A
Current at maximum power point (I_{mp})	5.58 A
Number of cells/strings	96
Parallel strings	66
Series connected modules per string	5

This paper is organized: Section II describes an IEEE 13-bus system model and solar PV system, also explains the modeling of HIF. Section III explains the proposed methodology for detecting and classifying HIF, and the detailed description of feature extraction using DWT analysis is presented in section IV. Section V portrays the proposed LSTM and other intelligence classifiers such as KNN, SVM, JDT, and NB. The results obtained from MATLAB simulation of PV integrated power network and classification output of various classifiers are discussed in section VI with a conclusion and future scope of this work presented in the last section.

II. SYSTEM MODEL STUDIED

In this study, the proffered RNN classifier's classification performance was tested on an IEEE 13-bus network model with high impedance fault, symmetrical and unsymmetrical faults, switching events (heavy load and capacitor bank), and transformer current. The IEEE 13 bus network model shown in Figure 1 has been developed in MATLAB/Simulink software environment to integrate a 300 kW solar PV unit (operating under STC) and different load facilities. The test system is interconnected with the primary grid source (100 MVA, 25 kV, 60 Hz) through an interconnecting transformer (200 kVA, 4.16 kV/25 kV). The detailed modeling of transmission line parameters and the load was given in [30]. The performance of the proposed RNN based classifier was evaluated while identifying HIF under normal conditions, switching events (capacitor bank and heavy load), transformer inrush current, and abnormal conditions (symmetrical and unsymmetrical faults: single line ground, double line, double line to ground and three-phase fault).

A. DESCRIPTION OF SOLAR PV SOURCE

The 300 kWp solar PV includes 3 (100 kW each) PV units. The specification of each solar cell used in the PV array

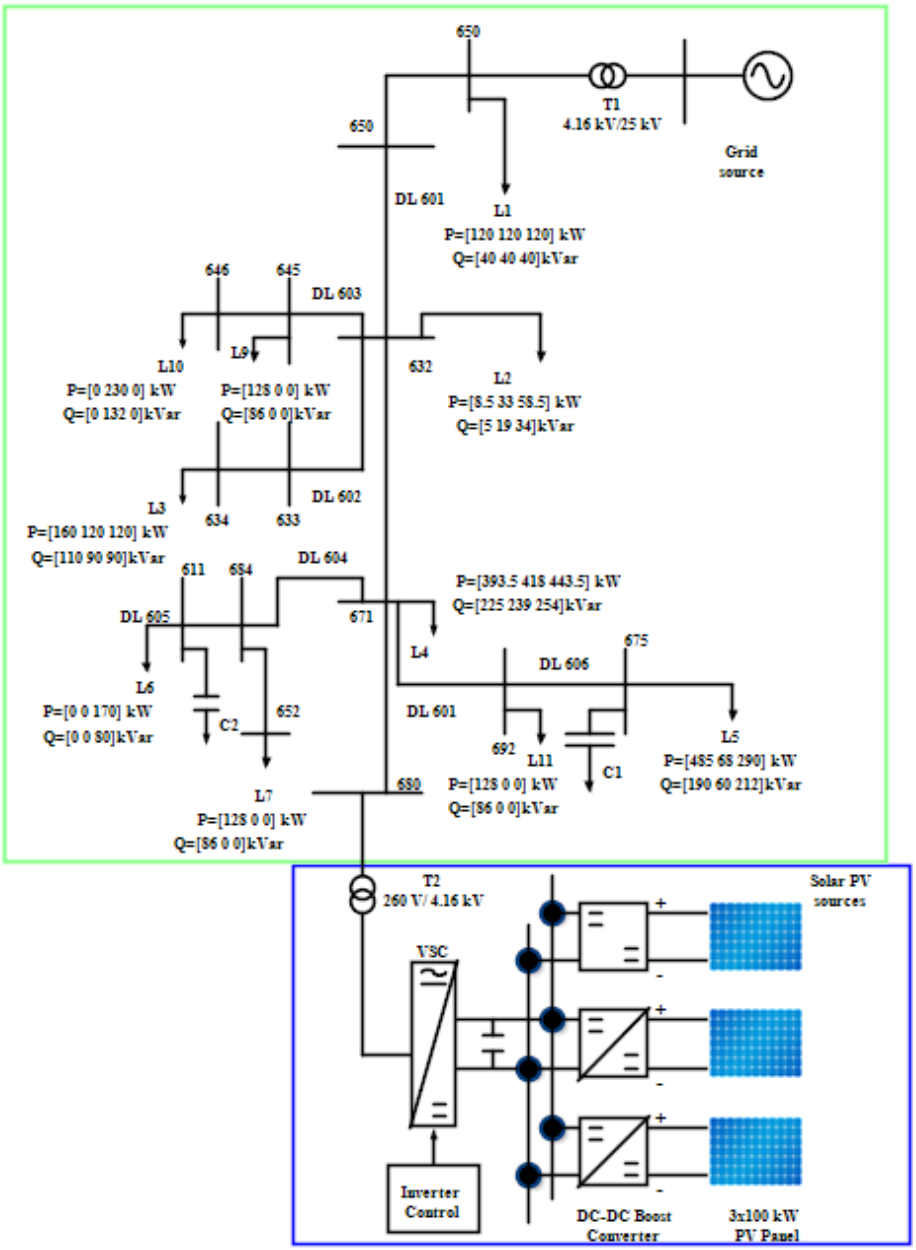

FIGURE 1. IEEE 13-bus system with the solar PV system.

and the PV array's configuration detail is listed in Table 1. The current and power level of a single solar cell (concerning the voltage) at different solar irradiance (W/m^2) conditions is portrayed in Figures 2(a) and 2(b), respectively. The PV system comprises a DC-DC boost converter and DC-AC VSI. The boost converter steps up the PV unit's output voltage (280 V DC at maximum power point) to 500 V. An incremental conductance method of the MPPT controller was used to adapt the DC-DC boost's duty cycle converter concerning solar irradiance for tracking the maximum power from the panel. A 3 level IGBT bridge circuit with PWM control (switching frequency of 1980 Hz) of PV inverter (VSI) system was considered. The inverter has two control loops (outer voltage and inner current control loop to regulate the output AC voltage) based on synchronous reference frame theory. The conventional proportional-integral controller was used in both the control loops of the inverter with the proportional (K_p) and integral (K_i) gain values of the outer controller: $K_p = 7$ and $K_i = 800$ and inner controller: $K_p = 0.3$ and $K_i = 20$, respectively. Inverter's output voltage is 260 V AC, stepped up using a step-up transformer (200 KVA, 4.16 kV/260 V) to 4.16 kV for interconnecting into IEEE-13 bus power system network.

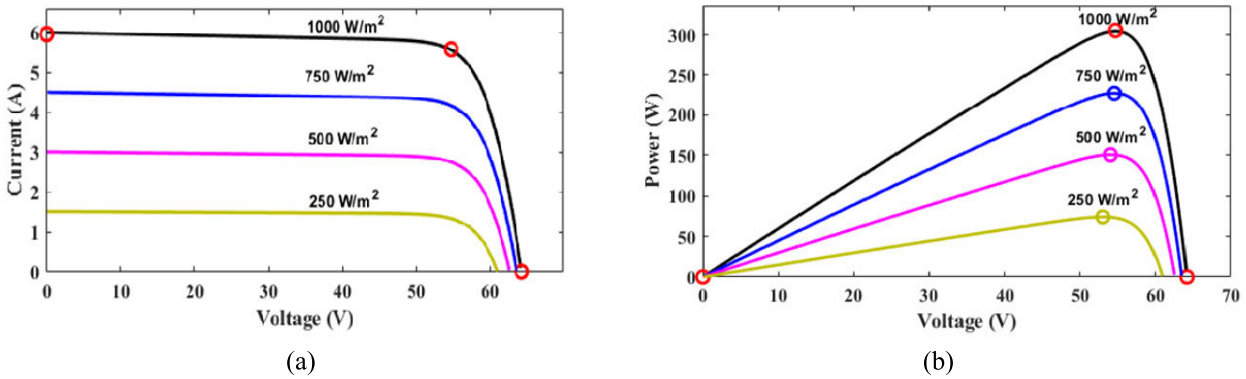

FIGURE 2. (a) I-V characteristics of PV array (b) P-V characteristics of PV array.

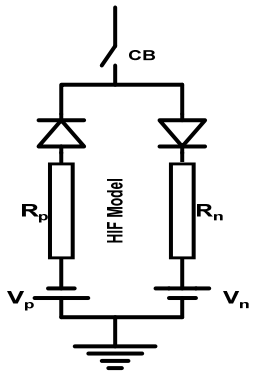

FIGURE 3. HIF model.

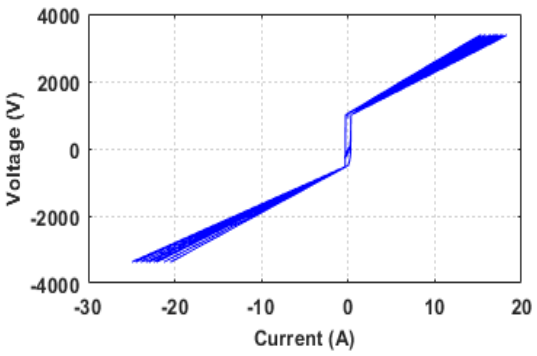

FIGURE 4. V-I characteristics of HIF model for varying V_p, V_n, R_p, and R_n.

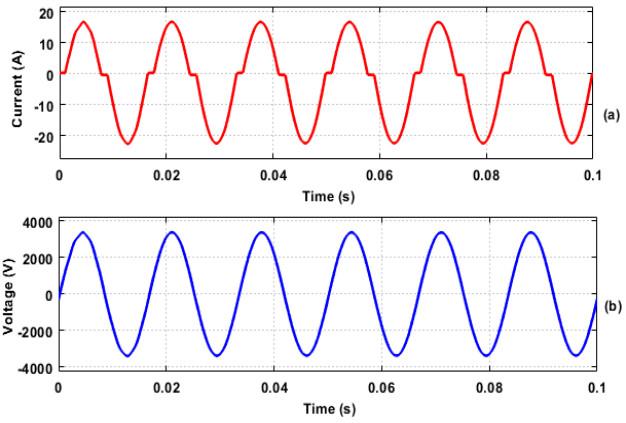

FIGURE 5. (a) Current at HIF location (b) Voltage at HIF location.

B. HIGH IMPEDANCE FAULT MODEL

The HIF occurs when a broken live overhead conductor has contact with a high resistive surface such as sand, asphalt, and tree, exhibiting non-linearity, randomness, asymmetry, shoulder, buildup, and intermittence [31]. HIF current waveform properties are modeled using an anti-parallel diode model depicting the HIF model's natural form based on the Emanuel model [3], [32] as given in Figure3. Using this model, the V-I characteristics of HIF are obtained by varying V_p, V_n, R_p, and R_n of HIF model between 500 to 8000 V, 1000 to 10000V, 120 to 5000 Ω, and 120 to 5000 Ω, respectively as depicted in Figure 4. The current and voltage waveform of HIF recorded with $V_p = 500$V, $V_n = 1000$ V, $R_p = R_n = 120\Omega$ is shown in Figure 5. It is observed that the current waveform shows non-linearity, asymmetry, and harmonic content for the HIF model considered. Further, the current waveform at the HIF location was analyzed using FFT analysis and found that second and third-order harmonic contents of 3.94% and 11.7%, respectively, with the overall THD range of 14.6 % represented in Figure 6.

III. PROPOSED METHODOLOGY

This section presents the detection and identification of HIF using intelligent classifiers in solar PV integrated power network. The detailed steps of the process of classification are portrayed in Figure 7 and also explained:

Step-1: Data Acquisition – In this case, the IEEE 13-bus system with solar PV network was simulated in MATLAB/Simulink and various fault conditions such as LG, LL, LLG, LLLG, and HIF. Then, each phase's current features during these conditions are recorded for feature extraction using DWT analysis. Further, the Non-fault event of capacitor

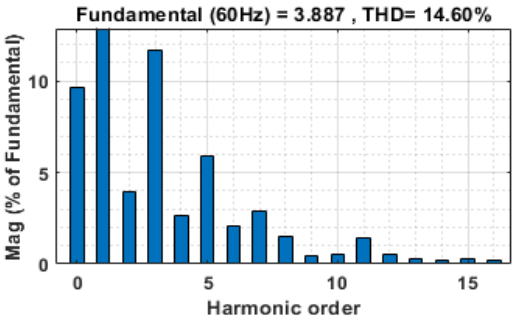

FIGURE 6. HIF current spectrum.

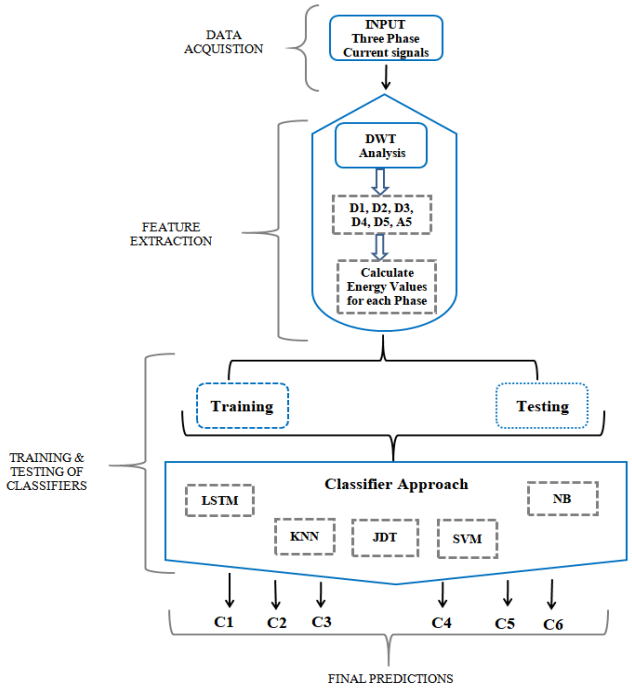

FIGURE 7. Schematic view of fault classification using intelligent classifiers.

switching, load switching, transformer inrush current, and change of irradiance of solar PV were considered normal operating conditions of the system as the protective relay is insensitive to changes.

Step-2: Feature Extraction –During this phase, DWT is used to transform the time domain current signal (during faulty and non-faulty conditions) into a time-frequency domain signal by decomposition. Different characteristics have been observed from the decomposed current signal with large coefficients in different frequency bands during the disturbances. The extraction of features (energy value) from all these frequency bands is applied to give good discrimination results from the classifiers.

Step-3: Training Phase –The extracted energy values under different system operating conditions are used to train the intelligent classifiers. A total data set of 970 data samples were obtained by varying the fault resistances from 20 Ω to 150 Ω in step 10 Ω during LG, LL, LLG, and LLLG type of fault. Further, the perturbation of R_p, R_n, V_p, and V_n in the HIF model whose information are detailed in Section 2.2 and for the case of normal operating conditions: capacitor switching from 300 kVar to 500 kVar in the step of 50kVar, load switching of 0.5 MW to 2 MW in the step of 0.25 MW, transformer inrush current by switching the transformer of 4.16 kV/480 V at various buses, and change in irradiations of the solar PV system from 750 to 1000 W/m^2 were considered for collecting the data samples to train the classifier.

Step-4: Prediction Phase –In this condition, 20% of the data sample was used to test the intelligent classifiers such as LSTM, KNN, DT, SVM, and NB to identify different events that occur in the developed power network.

IV. FEATURE EXTRACTION USING DWT ANALYSIS

Wavelet transform is one of the most widely used signal processing tools for detecting the low amplitude, short duration, fast decaying and oscillating type of signals or transients encountered in the power system during a fault or any other abnormal conditions [12]. The main feature of the wavelet function is localization in both the time and frequency domain. Hence, it applies to wideband signals that are non-periodic and comprises both sinusoidal and impulse components, as seen in fast power system transients [3]. In general, the WT exists in two forms: continuous and discrete WT. The CWT has limitations of low redundancy during the signal's reconstruction, and hence DWT was used for practical application. Thus, the DWT can be mathematically defined for signal $x(n)$ as:

$$DWT(m,k) = \frac{1}{\sqrt{a_0^m}} \sum_n x(n) * h\left(\frac{k - na_0^m}{a_0^m}\right) \quad (1)$$

where a_0^m and na_0^m are the scaling and translation parameters, n and m are the integer variables, and h is the mother wavelet, k is an integer value that defines the particular sample number in an input signal. The sampling frequency of 20 kHz and mother wavelet of db4 was chosen for extracting the energy value features to train the classifier. The detailed explanation of mother wavelet choice, selection of sampling frequency, number of levels, and bandwidth for each level are reported in the previous work of authors in [3], [12].

A. ENERGY VALUES

The feature extraction was carried out to reduce the raw signal's voluminous data to be analyzed. In this work, an energy value (EV) was calculated from the detail coefficients and approximations level of wavelet coefficients defined as [3]:

$$EV = \sum_{i=1}^{k} \left[|D_i|^2\right] + |A_k|^2 \quad (2)$$

k depicts the number of levels and is chosen as 5, d_1, d_2, d_3, d_4, and d_5 represents the detailed coefficient level and a_k is approximations of the signal's final level.

V. MATERIALS AND METHODS OF CLASSIFICATION

This fragment describes the various classifier approaches such as KNN, DT, SVM, NB, and the proposed LSTM recurrent network used to detect and classify the HIF and other symmetrical and unsymmetrical faults that occur in the PV integrated power network developed in MATLAB/Simulink software environment. In a classification of different fault events using disparate classifiers with an assumption of system condition as several classes labeled: C1-Non-faulty event, C2-HIF, C3- Single line to ground fault (LG), C4- Double line fault (LL), C5-Double line to ground fault (LLG) and C6- Three-phase fault (LLLG).

A. LONG SHORT-TERM MEMORY (LSTM) RNN

In recent years, the development of deep learning methods has laid down the RNN as one of the most state-of-art models for classification problems applied to sequential data. The RNN is a particular form of standard artificial neural network (ANN) with feedback loops to store the recent input events as activation. Further, capable of creating a correlation between the current and preceding information in the network. However, the RNN can also learn any length but suffer from limitations of gradient exploding and vanishing [26]–[28]. This can be overcome by the particular form of RNN proposed by Hochreiter and Schmidhuber (1997), in which RNN cell is replaced by a gated cell called Long Short-Term Memory network. The basic architecture of a single LSTM network is portrayed in Figure 8.

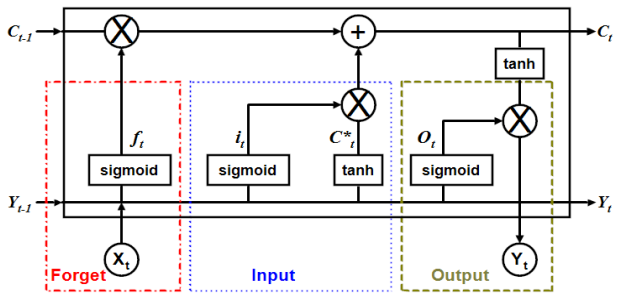

FIGURE 8. Single LSTM cell architecture with gates [26].

An LSTM network comprises a memory cell illustrated by C_t with self-loops, storing the temporal information encoded on the cell state. Three gates, namely control the flow of information in the network: forget gate $f_t \epsilon [0, 1]$, Input gate $i_t \epsilon [0, 1]$, and output gate $O_t \epsilon [0, 1]$. During training, the network learns what needs to be memorized and when to allow reading/writing to minimize the misclassification rate. In particular, the Forget gate determines what information from the last memory cell state is expired and should be removed. The input gate updates the cell state by selecting appropriate information from candidate memory cell state C^*_t. The output gate filters the information from the memory cell so that the model considers only the critical information for the prediction task. The value of each gate is determined as follows [26]–[29],

$$\left\{ \begin{array}{l} i_t = sigmoid(W_i[y_{(t-1)}, X_t] + b_i) \\ f_t = sigmoid(W_f[y_{(t-1)}, X_t] + b_f) \\ C^*_t = sigmoid(W_C[y_{(t-1)}, X_t] + b_C) \\ O_t = sigmoid(W_O[y_{(t-1)}, X_t] + b_O) \end{array} \right\} \quad (3)$$

$W_{[i,f,C,O]}$ are the weight matrices and $b_{[i,f,C,O]}$ are the network's bias vectors. The memory cell value (C_t) and output (y_t) of the network is obtained using the equations as follows,

$$\left\{ \begin{array}{l} C_t = C_{(t-1)}.f_t + C^*_t.i_t \\ y_t = O_t * tanh(C_t) \end{array} \right\} \quad (4)$$

The proposed LSTM network was trained with 970 samples of EV data extracted using DWT analysis of current signal under different operating conditions such as standard, LG, LL, LLG, LLLG, and HIF. The training data is obtained by changing fault resistances during LG, LL, LLG, and LLLG type of fault. Also, the perturbation of R_p, R_n,V_p, and V_n in the HIF model and for the case of non-faulty conditions: capacitor switching, load switching, transformer inrush current, and change of irradiations were considered.

B. K-NEAREST NEIGHBOR ALGORITHM (KNN)

KNN is a well-known non-parametric classification technique that gives high classification accuracy for a problem with non-nominal and unknown distributions. It exhibits lazy learning by imparting less effort during training and full effort during the prediction phase. The classification task is performed based on similarity index by considering the distance measure in which 'k' refers to the integer value lies between 3 to 10 [33].Generally, it is preferable to select the odd value of 'k,' and the classifier's output is predicted based on majority votes cast by the neighbor class. In this work, the value of k is chosen as 3, and the output for any test case X, the probability of X belonging to class C_i should be maximum, which can be defined as:

$$KNN(X) = maxP(C_i, X) \quad (5)$$

where $P(C_i, X)$ is the probability of X in class C_i. The nearest neighbors' weights are assigned based on Euclidean distance and are defined in [34].

C. J48 DECISION TREE

The J48 decision tree algorithm follows the rule of C4.5.It is a widely used algorithm since it has the features of high reliability, easy implementation, can manage easily with large data quantities, and data set with missing values [35]. In general, the JDT has the following elements: branches, nodes, leaves, and roots. The decision tree is used to classify the input feature vectors with a process that starts from tree root to identification of leaf node, and it works based on the highest entropy reduction. At each node of the tree, training instances are passed into the branch and the value of test attributes. Also, the subset of training instances is used recursively to generate the new type of nodes. During the case of no change in the output value, that output attribute is assigned for the

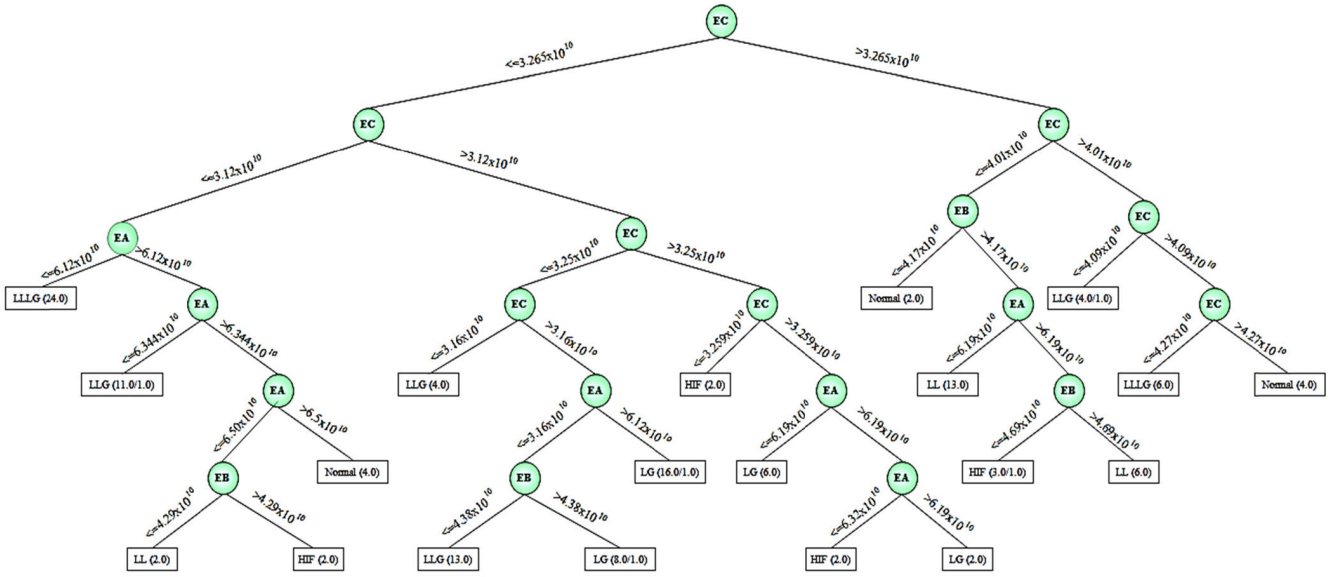

FIGURE 9. Decision Tree based on energy value feature.

same class value, and a leaf is generated to end the nodes' recursion. When there are no instances pass through, a leaf node is generated with a typical class value for the output attributes [36]. Finally, creating nodes continues recursively until all the instances are exhausted. During the classification process with JDT, the following factors are considered [37], Confidence factor: The parameter of minimum value (0.25) has been assigned for confidence factor to perform pruning in DT, in such a way to remove any branch which does not meet the ratio between the correctly and incorrectly classified instances.

- The minimum number of leaf-level: Assigned level 2 for the instances of DT and the value of fold parameter of 3 (determines the amount of data used for reducing the pruning error)
- For the pruned tree, 7 numbers trees and 4 leaves have been considered.

Thus, the DT for detecting HIF and other fault events of the PV integrated power network is shown in Figure 9.

D. SUPPORT VECTOR MACHINE

The SVM is a well-known data-driven technique framed using statistical learning theory. It was introduced by Vapnik et al. as a binary classifier for the classification of linear and non-linear data. The SVM finds an optimal hyperplane to separate the data set into two distinct classes {-1, +1}. This is done by mapping the linearly inseparable input data set to a high dimensional feature space through a kernel function K(u_i,u_j). Thus, it increases data dimensionality by feature mapping, which helps construct the hyperplane separating the classes [8], [12]. The misclassification of classifiers can be avoided by maximizing the margin between the two data sets through the hyperplane, as depicted in Figure 10. The hyperplane that separate different classes of data can be defined as,

$$f(x) = W^T x + b \tag{6}$$

where,

$$x \in \left\{ \begin{array}{l} ClassI, if\ f(x) = +1 \\ ClassII, if\ f(x) = -1 \end{array} \right\}$$

$f(x)$ is a linear hyperplane function with bias b, data points x, and weight vector w, obtained via training [13]. The most commonly used kernel functions are linear, polynomial, radial basis function (RBF), and sigmoid. In this work, an RBF reduces the search space of parameter sets and gives a better accuracy rate than other functions [12], [13].The various procedures used to classify data using multi-class SVM are one-against-all, one-against-one, and a directed acyclic graph method. It was proved that the one-against-one method is the best choice for practical applications with maximum accuracy. Therefore, this work also adopts a one-against-one method to classify faults and is implemented using the LIBSVM toolbox in MATLAB.

E. NAÏVE BAYES

NB is an extensively used statistics classifier for classifying the linear and non-linear data because of its simplicity and no parameter adjustment. NB is based on Bayes' theorem with an assumption of class conditional independence among the features. The NB classifier will modify the marginal probability of an event according to some extra information, given that the attributes have independent properties and are of equal importance. Initially, the classifier calculates the probabilities of unclassified data corresponding to each class and then classifies this data into the class having the

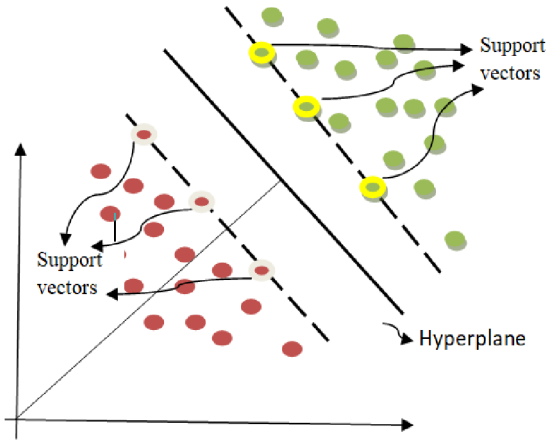

FIGURE 10. Support vector machine.

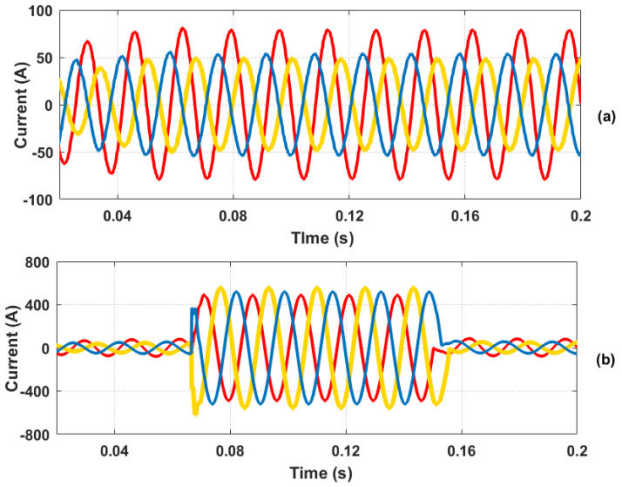

FIGURE 11. Non-faulty event (a) Normal condition (b) Load switching.

highest probability. For classification, a prior distribution is provided for each attribute in the class during the training stage. In the testing phase, the classifier gives probabilities of all the classes to which one testing instance belongs, and then the class having the maximum probability of testing data was set. The posterior probability of C at any instance of X can be defined using Bayes' theorem as [38], [39]:

$$P(C|X) = \frac{P(C).P(X|C)}{P(X)} \tag{7}$$

where P(C) is the prior probability, P(X|C) is the likelihood of $C = [C_1, C_2, \ldots C_j]$ concerning $X = \{x_1, x_2, \ldots x_k\}$, j is the number of fault classes (Normal, HIF, LG, LL, LLG, and LLLG) and k is the attributes of data (Energy values). The prediction is made for the class with the highest posterior probability as [24], [35]:

$$C_N B = argmax P(C) \prod_{i=1}^{k} P(X_i|C) \tag{8}$$

F. PERFORMANCE INDICES

The performance of intelligence classifiers has been evaluated using various indices:

Kappa Statistics (KS): It is an alternative measure of classifiers' accuracy, which signifies an agreement between the observed and expected type of fault in the system. The performance of classifier can vary based on KS value: KS = 1 (excellent); KS = 0.4 to 0.75 (good); KS = less than 0.4 (poor). The KS index is defined as [12], [27].:

$$\text{KS} = \frac{\text{Observed Fault} - \text{Expected Fault}}{1 - \text{Expected fault}} \tag{9}$$

Precision (P): It is the division of correctly predicted positive observations between the total predicted positive observations and is given as follows [27]:

$$\text{Precision} = \frac{T_P}{T_P + F_P} \tag{10}$$

where T_P is the true positive and F_P is the false positive

Recall (R): The division of correctly predicted positive observations among the class's entire observations. It is expressed as [27],

$$\text{Recall} = \frac{T_P}{T_P + F_N} \tag{11}$$

F-measure: It is a weighted average of precision and recall, which is defined as [27],

$$\text{F} - \text{measure} = \frac{(2 \times P \times R)}{P + R} \tag{12}$$

where P is the Precision and R is the recall

VI. RESULTS AND DISCUSSION

This section describes the simulation results of the PV integrated IEEE 13-bus power network presented in section 2. For analysis, the fault is applied at different buses of the 13-bus system, and the data was collected for training and testing the classifiers. In this work, 80% of data was used for training, and 20% of data was used to test the classifiers. Initially, the network was simulated in MATLAB/Simulink, and the results were obtained during regular operation, a transient operation like load and capacitor switching, transformer inrush current, conventional faults such as LG, LL, LLG, and LLLG, and HIF occurrence. Figure 11(a) depicts the system's regular operation, and it is inferred that the current waveform is unbalanced for unbalanced loading of the power network.

For analysis of the non-faulty event, capacitor and load switching and transformer inrush current events were applied to the system during 0.066 s to 0.15 s. A capacitor switching of 300 kVar to 500 kVar in a step of 50kVar and load switching of 0.5 MW to 2 MW in the step of 0.25 MW were used for analysis. For instance, 1 MW of load and 300 kVar switching of capacitor switching during 0.066s to 0.15 s are shown in Figure 11(b) and 12(a), respectively. It is seen that the initial transients are high during CS, and the magnitude of current increases during these switching transients. On the other side,

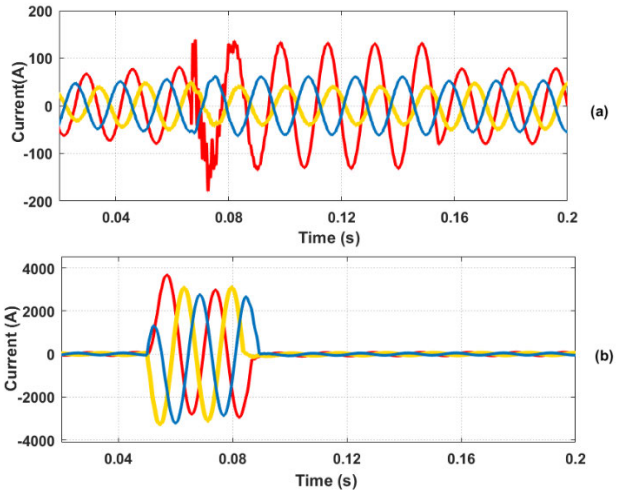

FIGURE 12. Non-faulty event (a) Capacitor switching (b) Transformer In-rush current.

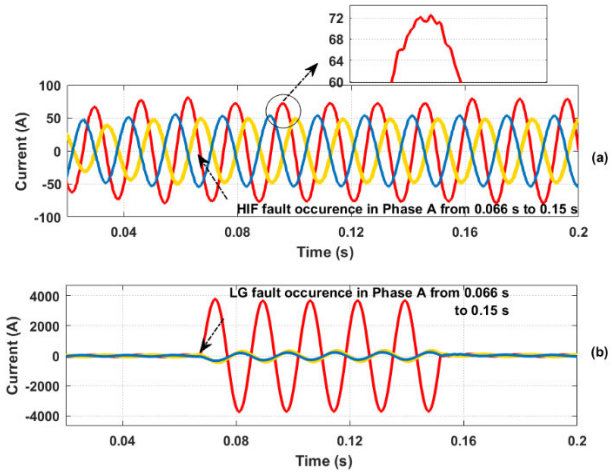

FIGURE 13. Fault condition (a) HIF (b) LG fault.

the switching of the 4.16 kV/480 V transformer results in a high inrush current, as shown in Figure 12 (b).

The transformer's switching has been done at various locations of the 13-bus system, and then the current signal is recorded for further analysis. For analyzing low and high impedance fault events, different faults were applied with the fault inception angle of 0° and 45°, for illustration the occurrence of HIF and LG fault in Phase A of the three-phase system (with an inception angle $\theta_f = 0°$) are shown in Figure 13(a) and 13(b), respectively. It is observed that the magnitude of fault current is high during the occurrence of LG fault. On the flip-side, the magnitude of HIF current varies for different fault resistance considered in the two diode models assumed as given in Figure 3. The current magnitude is higher or lower than the load current based on HIF parameters' assumed value. In the proposed study, the model considers the worst-case scenario of HIF, whose magnitude of fault

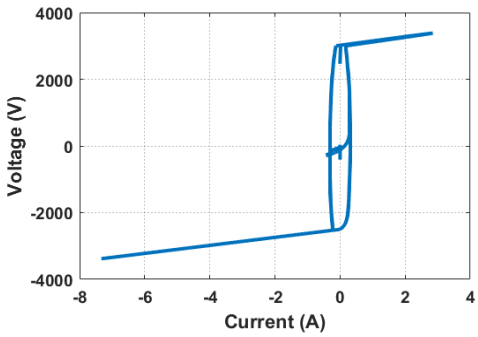

FIGURE 14. V-I characteristics of HIF model ($V_p = 500V$, $V_n = 1000$ V, $R_p = R_n = 120\ \Omega$).

current is limited to be less than 10% of actual load current. Figure 13(a) represents the fault current waveform due to HIF (with following parameters: $R_p = 120\ \Omega$, $R_n = 120\ \Omega$, $V_p = 3000$ V, and $V_n = 2500$ V). The magnitude of fault current is less than the load current depicting the worst-case scenario of HIF. The HIF model's V-I characteristic recorded during this case shows the non-linear relationship between the voltage and current, as shown in Figure 14.

Further, irregularities in the HIF current (Figure 13 (a)) is masked substantially at the substation (i.e., IEEE 13-bus system). However, the low amplitude of HIF current with irregularities is a significant challenge to power engineers for designing the protection scheme to detect the HIF. Therefore, signal processing techniques were highly employed to extract the features from these signals, which have small changes in magnitude and help identify the events appropriately.

Therefore, DWT based SPT techniques were used to extract features to train and test the intelligent classifiers. This tool's strength lies in the fact that the DWT can detect and distinguish between infinitesimal wave-shape changes. The current waveform at the substation (13-bus system) during normal and HIF conditions looks similar. The current waveform at the substation during HIF may have slight disturbance, but extend of such distortion may change for several pre-fault conditions. On processing such signals using DWT analysis results in a more consistent signature.

For illustration, the DWT analysis of Phase A during regular operation, capacitor switching, LG fault, and HIF were shown in Figures 15 to 18. The result shows that the wavelet coefficients (d1 to d5, and a5) have shown appropriate changes corresponding to system operation. No spikes or peaks are detected in the DWT analysis wavelet coefficients in regular operation, as represented in Figure 15. In contrast, during CS, the magnitude of wavelet coefficients (d1 to d5) increases, as shown in Figure 16. Similarly, spikes have been detected in wavelet coefficients (d1 to d5) during LG and HIF occurrence, as given in Figures 17 and 18, respectively. However, the amplitude of peak is high during CS and less in HIF, but this value is greater than the system's regular operation. The low-impedance fault like LG has peaked in wavelet coefficients during the start and end period of fault

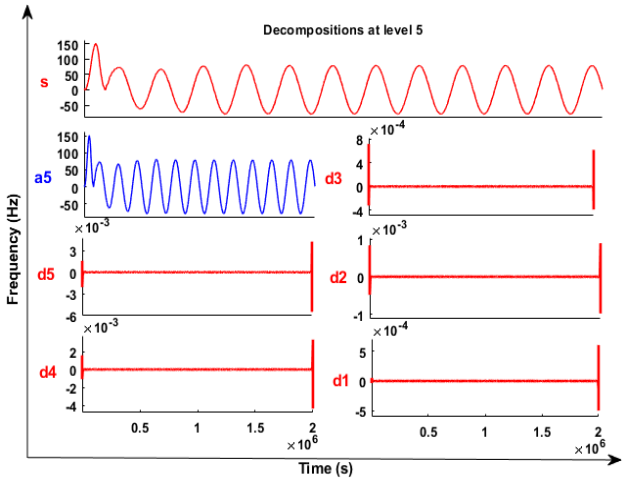

FIGURE 15. DWT analysis of Phase A during normal condition.

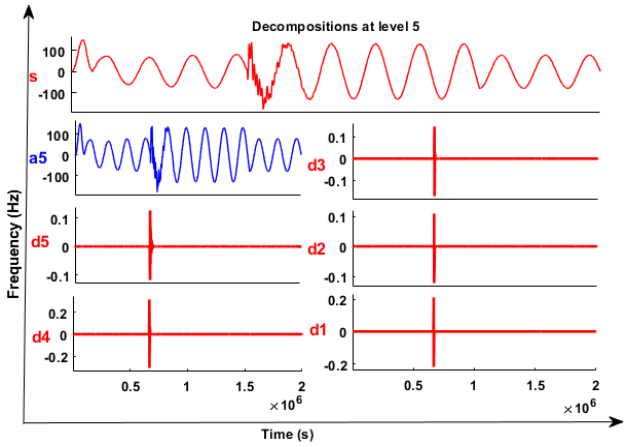

FIGURE 16. DWT analysis of Phase A during capacitor switching.

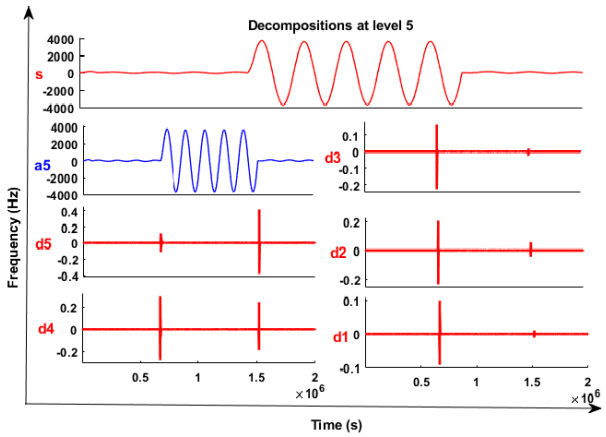

FIGURE 17. DWT analysis of Phase A during LG fault.

occurrence. Based on the value of spikes during different disturbances, an EV feature has been extracted for each phase of the three-phase system of the power network considered. Then, the obtained feature was used to train and test the classifiers to identify the disturbances appropriately.

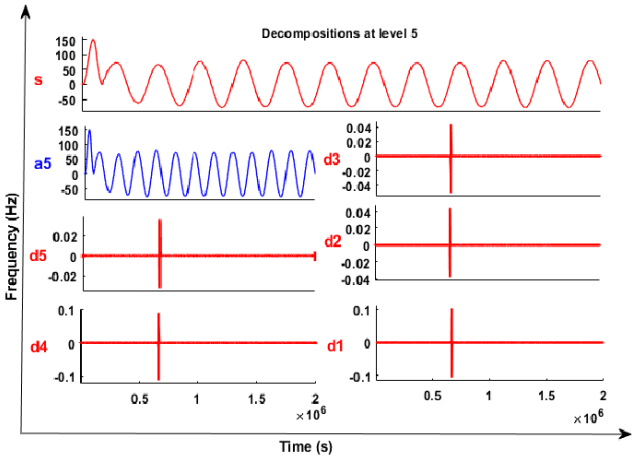

FIGURE 18. DWT analysis of Phase A during HIF.

TABLE 2. Confusion matrix during the training of LSTM network.

Classes	C1	C2	C3	C4	C5	C6
C1	**91**	21	0	0	0	0
C2	18	**246**	0	0	0	0
C3	0	0	**109**	2	8	1
C4	0	0	10	**110**	0	0
C5	0	0	0	0	**116**	4
C6	0	0	0	0	0	**40**

A. CLASSIFICATION USING INTELLIGENT CLASSIFIERS

Here, the different system condition was analyzed by assuming different classes: C1-Non-faulty event, C2-HIF, C3- Single line to ground fault (LG), C4- Double line fault (LL), C5-Double line to ground fault (LLG) and C6- Three-phase fault (LLLG). An RNN based LSTM network was proposed to detect and classify the HIF from other low-impedance fault disturbances (symmetrical and unsymmetrical fault) and switching transients in PV integrated IEEE 13-bus power network. The input data of 970 data samples were used for training the LSTM classifier, and the details of predictions during training are given in Table 2. For testing the classifiers, a 20% data set (194 data samples) was used, and the predictions obtained during this case are illustrated using a confusion matrix given in Table 3. The classification accuracy (CA) during testing and training is shown in Figure 19 and is calculated using (13).It is seen that the proposed LSTM network obtain 91.23 % and 91.75 % accuracy during testing and training of classifier depicting its significant performance in classifying the events.

$$\text{CA} = \frac{\text{Number of fault events correctly identified}}{\text{Total number of events}} \times 100\% \tag{13}$$

Further, the study was extended to compare the proposed RNN based LSTM classifier's performance with other intelligent classifiers such as KNN, DT, SVM, and NB to

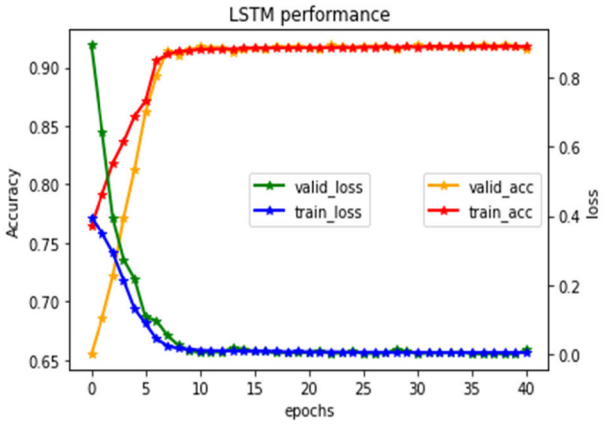

FIGURE 19. Performance Accuracy during training and testing of LSTM network.

TABLE 3. Confusion matrix during testing of proposed LSTM network.

Classes	C1	C2	C3	C4	C5	C6	System condition
C1	**21**	7	0	0	0	0	Non-faulty event
C2	5	**61**	0	0	0	0	HIF
C3	0	0	**28**	0	2	0	LG
C4	0	0	3	**27**	0	0	LL
C5	0	0	0	0	**30**	0	LLG
C6	0	0	0	0	0	**10**	LLLG

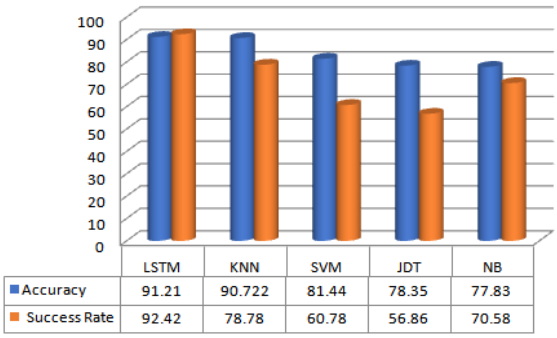

FIGURE 20. Accuracy and Success rate of classifiers.

detect HIF in PV integrated IEEE 13-bus power network. The training and testing of different classifiers were done as like LSTM network. For instance, the prediction of the KNN classifier during testing is shown in Table 4. The results of CA obtained by different classifiers are shown in Figure 20. The result shows that the proposed LSTM possesses higher accuracy of 91.21%, and the KNN performs to give 90.72%. The classifiers such as SVM, JDT, and NB have CA of 81.44%, 78.35 %, and 77.83 %, respectively. Figure 21 depicts the number of instances (53) misclassified by the NB classifier and a smaller number of instances (17) by the proposed classifier. The performances of other classifiers are not significantly appreciable except the KNN classifier. This inference

TABLE 4. Confusion matrix of KNN during testing.

Classes	C1	C2	C3	C4	C5	C6	System condition
C1	**25**	3	0	0	0	0	Non-faulty event
C2	3	**52**	3	7	0	1	HIF
C3	0	0	**30**	0	0	0	LG
C4	0	0	1	**29**	0	0	LL
C5	0	0	0	0	**30**	0	LLG
C6	0	0	0	0	0	**10**	LLLG

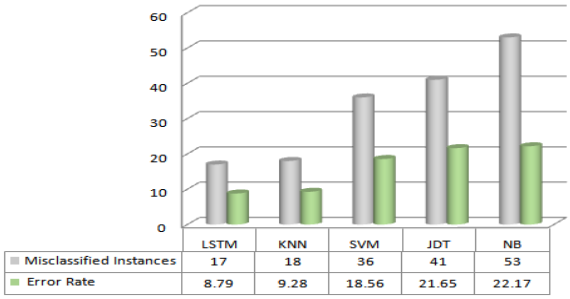

FIGURE 21. Misclassification instances and the error rate of classifiers.

was also interpreted as error rate defined as:

$$\text{Error Rate} = \frac{\text{Number of fault events incorrectly identified}}{\text{Total number of events}} \times 100\% \tag{14}$$

The proposed LSTM network has a minimum error rate of 8.79%, and NB has a maximum of 22.17 %, as portrayed in Figure 21. SVM and JDT have a moderate performance on the flip side, and KNN has 9.28% showing better response. In particular, the analysis was carried out to detect the number of HIF event correctly identified using the index:

$$\text{Success Rate} = \frac{\text{Number of HIF events detected}}{\text{Total number of HIF events}} \times 100\% \tag{15}$$

The result obtained in Figure 20 reveals that the proffered LSTM gives a maximum success rate of 92.42 % by identifying the HIF events in the 13-bus PV integrated power network. The performance was worst in the JDT classifier case and was comparatively good for other classifiers such as KNN, SVM, and NB.

B. PERFORMANCE ANALYSIS OF CLASSIFIERS

The classifier's robustness was further examined by evaluating the PI of Kappa Statistic (KS), Precision, Recall, and F-measure. Figure 22 portrays the KS index for all the intelligent classifiers used for fault classification. The proposed LSTM performs to give a maximum value of 0.891, and comparative performance was also observed in KNN of 0.882. On the flip-side, SVM, JDT, and NB give a moderate performance with the index value of 0.7637, 0.7205, and 0.7208, respectively. Thus, it is inferred that the classifier with a

TABLE 5. PI of different classifiers-precision index.

Class	Precision				
	LSTM	KNN	DT	SVM	NB
Non-faulty event	0.75	0.8928	0.7742	0.7097	0.8387
HIF	0.9242	0.7878	0.5686	0.6078	0.7059
LG	0.9333	1	1	1	0.6667
LL	0.9	0.9666	0.6818	0.7727	0.8636
LLG	1	1	0.8	0.9333	0.6667
LLLG	1	1	1	1	1

TABLE 6. PI of different classifiers-recall index.

Class	Recall				
	LSTM	KNN	DT	SVM	NB
Non-faulty event	0.8077	0.8928	0.8	1	1
HIF	0.8971	0.9454	0.8286	1	0.9231
LG	0.9032	0.8824	0.75	0.7317	0.8333
LL	1	0.8055	0.6818	0.7391	0.6786
LLG	0.9375	1	0.8	0.6087	0.6452
LLLG	1	0.909	0.8108	0.9677	0.6522

TABLE 7. PI of different classifiers- F-measure index.

Class	F-Measure				
	LSTM	KNN	DT	SVM	NB
Non-faulty event	0.7778	0.8929	0.7869	0.8302	0.9123
HIF	0.9104	0.8595	0.6744	0.7561	0.8
LG	0.9180	0.9375	0.8571	0.8451	0.7407
LL	0.9474	0.8787	0.6818	0.7556	0.7600
LLG	0.9677	1	0.8	0.7368	0.6557
LLLG	1	0.9524	0.8955	0.9836	0.7895

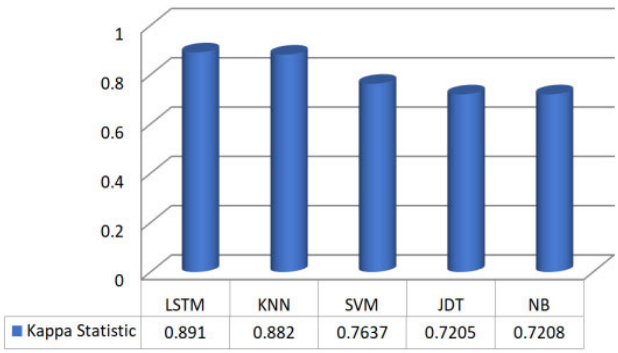

FIGURE 22. Kappa statistic performance of classifiers.

maximum value of KS index depicts excellent performance in classification, which is observed in the proposed RNN based LSTM network.

Further, the precision index depicted in Table 5 presents the CA obtained by the classifier for each event. It is seen that the proffered technique identifies several HIF events compared to other classifiers presented. Similarly, the other indices such as Recall and F-measure were measured, and the performance was observed to be superior for the proposed classifier than other classification approaches as presented in Table 6 and 7. Further, to validate the proposed classifier's performance, the fault detection time was compared for each classifier (LSTM, KNN, DT, SVM, and NB: 76 ms, 81.5 ms, 110 ms, 80 ms, and 82 ms, respectively). The time includes the SPT of DWT analysis and fault detection by the classifier. The results reveal that the proposed deep learning method of recurrent LSTM classifier detects quickly compared to other intelligent classifiers. The results of detection time were taken in a personal computer with the following specifications: 32-bit OS with x64-based processor (Intel (R) core (TM) i5-2410M CPU @2.30 GHz) and has memory capacity of 8 GB.

VII. CONCLUSION

The HIF procedure's detection relies on various conditions, some of which are network-specific and present exclusive characteristics. In this work, a more realistic PV-integrated IEEE 13-bus system was considered for the HIF study using the proposed RNN based LSTM network. Initially, the 13-bus distribution network was developed in MATLAB/Simulink to introduce various events (Non-faulty events: Normal operation, transformer inrush current, load switching, and capacitor switching, faulty-events: HIF, LG, LL, LLG, and LLLG). The three-phase current signal under these conditions was analyzed using DWT analysis with the mother wavelet of db4. The wavelet coefficients (d1, d2, d3, d4, d5, and a5) obtained was used to extract the energy value features for various phases to train and test the classifiers. The classifiers' result shows that the proposed RNN based LSTM performs better to give the classification accuracy of 91.21 % than other classifiers such as KNN, SVM, JDT, and NB.

Further, the success rate on detecting specific HIF events was 92.42 % for the proffered technique, and the rate was reasonably good for other classifiers presented. The PI of KS, precision, recall, and F-measure were also examined to validate different classifiers' robustness. The result shows that the propounded LSTM classifier outperforms significantly in terms of all PI and also detects the fault quickly compared to other classification approaches. The detection of HIF using advanced signal processing techniques and the hybrid classifier method is the future scope of the presented work.

REFERENCES

[1] M. Manohar, E. Koley, and S. Ghosh, "Reliable protection scheme for PV integrated microgrid using an ensemble classifier approach with real-time validation," *IET Sci., Meas. Technol.*, vol. 12, no. 2, pp. 200–208, Mar. 2018.

[2] B. K. Chaitanya, A. Yadav, and M. Pazoki, "An intelligent detection of high-impedance faults for distribution lines integrated with distributed generators," *IEEE Syst. J.*, vol. 14, no. 1, pp. 870–879, Mar. 2020.

[3] V. Veerasamy, N. I. Abdul Wahab, A. Vinayagam, M. L. Othman, R. Ramachandran, A. Inbamani, and H. Hizam, "A novel discrete wavelet transform-based graphical language classifier for identification of high-impedance fault in distribution power system," *Int. Trans. Electr. Energy Syst.*, vol. 30, no. 6, pp. 1–24, Jun. 2020.

[4] F. Xiao, T. Lu, M. Wu, and Q. Ai, "Maximal overlap discrete wavelet transform and deep learning for robust denoising and detection of power quality disturbance," *IET Gener., Transmiss. Distrib.*, vol. 14, no. 1, pp. 140–147, Jan. 2020.

[5] M. V. Reddy and R. Sodhi, "A rule-based S-transform and AdaBoost based approach for power quality assessment," *Electr. Power Syst. Res.*, vol. 134, pp. 66–79, May 2016.

[6] Z. Huo, Y. Zhang, P. Francq, L. Shu, and J. Huang, "Incipient fault diagnosis of roller bearing using optimized wavelet transform based multi-speed vibration signatures," *IEEE Access*, vol. 5, pp. 19442–19456, 2017.

[7] S. Roy and S. Debnath, "PSD based high impedance fault detection and classification in distribution system," *Meas. J. Int. Meas. Confed.*, vol. 169, Feb. 2021, Art. no. 108366.

[8] K. Thirumala, M. S. Prasad, T. Jain, and A. C. Umarikar, "Tunable-Q wavelet transform and dual multiclass SVM for online automatic detection of power quality disturbances," *IEEE Trans. Smart Grid*, vol. 9, no. 4, pp. 3018–3028, Jul. 2018.

[9] I. Baqui, I. Zamora, J. Mazón, and G. Buigues, "High impedance fault detection methodology using wavelet transform and artificial neural networks," *Electr. Power Syst. Res.*, vol. 81, no. 7, pp. 1325–1333, Jul. 2011.

[10] K. Sekar and N. K. Mohanty, "A fuzzy rule base approach for high impedance fault detection in distribution system using morphology gradient filter," *J. King Saud Univ.-Eng. Sci.*, vol. 32, no. 3, pp. 177–185, Mar. 2020.

[11] V. Veerasamy, N. A. Wahab, R. Ramachandran, M. Mansoor, M. Thirumeni, and M. L. Othman, "High impedance fault detection in medium voltage distribution network using discrete wavelet transform and adaptive neuro-fuzzy inference system," *Energies*, vol. 11, no. 12, p. 3330, Nov. 2018.

[12] V. Veerasamy, N. I. Abdul Wahab, R. Ramachandran, M. Thirumeni, C. Subramanian, M. L. Othman, and H. Hizam, "High-impedance fault detection in medium-voltage distribution network using computational intelligence-based classifiers," *Neural Comput. Appl.*, vol. 31, no. 12, pp. 9127–9143, Dec. 2019.

[13] M. Sarwar, F. Mehmood, M. Abid, A. Q. Khan, S. T. Gul, and A. S. Khan, "High impedance fault detection and isolation in power distribution networks using support vector machines," *J. King Saud Univ.-Eng. Sci.*, pp. 1–12, Jul. 2019.

[14] M. R. Lukowicz and L. Kang, "High-impedance fault detection in distribution networks with use of wavelet-based algorithm," *IEEE Trans. Power Del.*, vol. 21, no. 4, pp. 1793–1802, Oct. 2006.

[15] M. Y. Suliman and M. T. Ghazal, "Detection of high impedance fault in distribution network using fuzzy logic control," in *Proc. 2nd Int. Conf. Electr., Commun., Comput., Power Control Eng. (ICECCPCE)*, Feb. 2019, pp. 103–108.

[16] S. Wang and P. Dehghanian, "On the use of artificial intelligence for high impedance fault detection and electrical safety," *IEEE Trans. Ind. Appl.*, vol. 56, no. 6, pp. 7208–7216, Nov. 2020.

[17] V. Ashok and A. Yadav, "Fault diagnosis scheme for cross-country faults in dual-circuit line with emphasis on high-impedance fault syndrome," *IEEE Syst. J.*, early access, May 25, 2020, doi: 10.1109/JSYST.2020.2991770.

[18] Q. Cui, K. El-Arroudi, and Y. Weng, "A feature selection method for high impedance fault detection," *IEEE Trans. Power Del.*, vol. 34, no. 3, pp. 1203–1215, Jun. 2019.

[19] Y. Zhang, X. Wang, J. He, Y. Xu, F. Zhang, and Y. Luo, "A transfer learning-based high impedance fault detection method under a cloud-edge collaboration framework," *IEEE Access*, vol. 8, pp. 165099–165110, 2020.

[20] A. Soheili, J. Sadeh, and R. Bakhshi, "Modified FFT based high impedance fault detection technique considering distribution non-linear loads: Simulation and experimental data analysis," *Int. J. Electr. Power Energy Syst.*, vol. 94, pp. 124–140, Jan. 2018.

[21] X. Wang, J. Gao, X. Wei, G. Song, L. Wu, J. Liu, Z. Zeng, and M. Kheshti, "High impedance fault detection method based on variational mode decomposition and Teager–Käiser energy operators for distribution network," *IEEE Trans. Smart Grid*, vol. 10, no. 6, pp. 6041–6054, Jan. 2019.

[22] Y.-S. Oh, J. Han, G.-H. Gwon, D.-U. Kim, C.-H. Noh, C.-H. Kim, T. Funabashi, and T. Senjyu, "Detection of high-impedance fault in low-voltage DC distribution system via mathematical morphology," *J. Int. Council Electr. Eng.*, vol. 6, no. 1, pp. 194–201, Jan. 2016.

[23] M. Mishra and P. K. Rout, "Detection and classification of micro-grid faults based on HHT and machine learning techniques," *IET Gener., Transmiss. Distrib.*, vol. 12, no. 2, pp. 388–397, Jan. 2018.

[24] E. Aker, M. L. Othman, V. Veerasamy, I. Aris, N. I. A. Wahab, and H. Hizam, "Fault detection and classification of shunt compensated transmission line using discrete wavelet transform and Naïve Bayes classifier," *Energies*, vol. 13, pp. 1–24, Jan. 2020.

[25] M. Kavi, Y. Mishra, and M. Vilathgamuwa, "Challenges in high impedance fault detection due to increasing penetration of photovoltaics in radial distribution feeder," in *Proc. IEEE Power Energy Soc. Gen. Meeting*, Jul. 2017, pp. 1–5.

[26] A. Y. Appiah, X. Zhang, B. B. K. Ayawli, and F. Kyeremeh, "Long short-term memory networks based automatic feature extraction for photovoltaic array fault diagnosis," *IEEE Access*, vol. 7, pp. 30089–30101, 2019.

[27] N. Qu, Z. Li, J. Zuo, and J. Chen, "Fault detection on insulated overhead conductors based on DWT-LSTM and partial discharge," *IEEE Access*, vol. 8, pp. 87060–87070, 2020.

[28] Z. Chang, Y. Zhang, and W. Chen, "Electricity price prediction based on hybrid model of adam optimized LSTM neural network and wavelet transform," *Energy*, vol. 187, Nov. 2019, Art. no. 115804.

[29] Y. Liu, L. Guan, C. Hou, H. Han, Z. Liu, Y. Sun, and M. Zheng, "Wind power short-term prediction based on LSTM and discrete wavelet transform," *Appl. Sci.*, vol. 9, no. 6, p. 1108, Mar. 2019.

[30] R. Azim, F. Li, Y. Xue, M. Starke, and H. Wang, "An islanding detection methodology combining decision trees and Sandia frequency shift for inverter-based distributed generations," *IET Gener., Transmiss. Distrib.*, vol. 11, no. 16, pp. 4104–4113, Nov. 2017.

[31] M. Mishra and R. R. Panigrahi, "Taxonomy of high impedance fault detection algorithm," *Meas. J. Int. Meas. Confed.*, vol. 148, Dec. 2019, Art. no. 106955.

[32] S. Kavaskar and N. K. Mohanty, "Detection of high impedance fault in distribution networks," *Ain Shams Eng. J.*, vol. 10, no. 1, pp. 5–13, Mar. 2019.

[33] M. Manohar, E. Koley, Y. Kumar, and S. Ghosh, "Discrete wavelet transform and kNN-based fault detector and classifier for PV integrated microgrid," in *Advances in Data and Information Sciences* (Lecture Notes in Networks and Systems), vol. 38. Singapore: Springer, 2018, pp. 19–28.

[34] D. Dou and S. Zhou, "Comparison of four direct classification methods for intelligent fault diagnosis of rotating machinery," *Appl. Soft Comput.*, vol. 46, pp. 459–468, Sep. 2016.

[35] D. Tien Bui, B. Pradhan, O. Lofman, and I. Revhaug, "Landslide susceptibility assessment in vietnam using support vector machines, decision tree, and Naïve Bayes models," *Math. Problems Eng.*, vol. 2012, pp. 1–26, 2012.

[36] U. Bashir and M. Chachoo, "Performance evaluation of J48 and Bayes algorithms for intrusion detection system," *Int. J. Netw. Secur. Appl.*, vol. 9, no. 4, pp. 1–11, Jul. 2017.

[37] N. A. Muhamad, I. V. Musa, Z. A. Malek, and A. S. Mahdi, "Classification of partial discharge fault sources on SF_6 insulated switchgear based on twelve by-product gases random forest pattern recognition," *IEEE Access*, vol. 8, pp. 212659–212674, 2020.

[38] E. Youn and M. K. Jeong, "Class dependent feature scaling method using Naïve Bayes classifier for text datamining," *Pattern Recognit. Lett.*, vol. 30, no. 5, pp. 477–485, Apr. 2009.

[39] S. H. Lu, D. A. Chiang, H. C. Keh, and H. H. Huang, "Chinese text classification by the Naïve Bayes classifier and the associative classifier with multiple confidence threshold values," *Knowl.-Based Syst.*, vol. 23, no. 6, pp. 598–604, 2010.

VEERAPANDIYAN VEERASAMY (Graduate Student Member, IEEE) received the bachelor's degree in electrical and electronics engineering from the Panimalar Engineering College, Chennai, India, in 2013, and the M.E. degree in power systems engineering from the Government College of Technology, Coimbatore, India, in 2015. He is currently pursuing the Ph.D. degree in power systems with Universiti Putra Malaysia, Malaysia. Since 2015, he has been working as an Assistant Professor with the Department of Electrical and Electronics Engineering, Rajalakshmi Engineering College, Chennai. His research interests include robust controllers for power system application, fault classification, power flow analysis, power system monitoring, deep learning classifiers, signal processing techniques, and Hopfield neural networks.

NOOR IZZRI ABDUL WAHAB (Senior Member, IEEE) graduated in electrical and electronic engineering from the University of Manchester Institute of Science and Technology (UMIST), U.K., in 1998. He received the M.Sc. degree in electrical power engineering from Universiti Putra Malaysia (UPM), in 2002, and the Ph.D. degree in electrical, electronic and system engineering from Universiti Kebangsaan Malaysia (UKM), in 2010. He is currently an Associate Professor with the Department of Electrical and Electronic Engineering, Faculty of Engineering, UPM. He has more than 100 publications (Journals: 20 local and 40 international, and Conference papers: 30 local and 20 international) under his name. His research interests include power system stability studies (dynamic and control), applying artificial intelligence in power systems, and power system quality. He is also a Researcher and the Founding Member of the Centre for Advanced Power and Energy Research (CAPER), UPM, and an Associate Member of the Centre of Electromagnetic and Lightning Protection Research (CELP), UPM. He is also a registered Chartered Engineer under the Engineering Council U.K. and the Institution of Engineering and Technology (IET) U.K., a Professional Engineer (Ir.) awarded by the Board of Engineers Malaysia (BEM), and a member of The Institution of Engineers Malaysia (IEM), the IEEE Power and Energy Society (IEEE-PES), the IEEE Computational Intelligence Society (IEEE-CIS), the Institution of Engineering and Technology (IET) U.K., and the International Rough Set Society (IRSS).

MOHAMMAD LUTFI OTHMAN (Senior Member, IEEE) received the B.Sc. degree *(magna cum laude)* in electrical engineering from The University of Arizona (UofA), Tucson, AZ, USA, in 1990, and the M.Sc. and Ph.D. degrees in electrical power engineering from the Universiti Putra Malaysia (UPM), Malaysia, in 2004 and 2011, respectively. He is currently an Associate Professor with the Department of Electrical and Electronics Engineering, Faculty of Engineering, Universiti Putra Malaysia. His research interests include, among others, numerical protective relay modeling, simulation, and operation analysis using computational-intelligent-based data mining and expert system approaches. His research interest also includes energy efficiency management studies. He is also a Researcher and the Founding Member of the Centre for Advanced Power and Energy Research (CAPER), UPM. He also practices as an Electrical Engineering Consultant in electrical services installation and works as an Electrical Director/Partner in a local engineering consulting firm. He is also a Professional Engineer (PEng) registered under the Board of Engineers Malaysia (BEM), a Chartered Engineer (CEng) registered under the Engineering Council U.K., a Registered Electrical Energy Manager (REEM) under Energy Commission Malaysia Certified Professional in Measurement and Verification (CPMV) under Malaysian Green Technology Corporation (under KETHHA), a Corporate Member of the Institution of Engineers Malaysia (IEM), a Senior Member of the IEEE Power and Energy Society (IEEE-PES) and the IEEE Computational Intelligence Society (IEEE-CIS), a member of the Institution of Engineering and Technology (IET) U.K., the International Rough Set Society (IRSS), the Asian Council of Science Editors (ACSE), the Academic keys Who's Who in Engineering Higher Education (WWEHE), and the International Rough Set Society (IRSS), a Graduate Technologist under the Malaysia Board of Technologist (MBOT), and a member of Phi Kappa Phi ($\Phi K \Phi$) Honor Society, The University of Arizona. His biographical profile is mentioned in the Marquis Who's Who in the World 2016 (33rd Edition). As a Professional Engineer, he is also a Mentor and Professional Interviewer for IEM/BEM Professional Engineer and the Engineering Council U.K. Chartered Engineer aspirants.

SANJEEVIKUMAR PADMANABAN (Senior Member, IEEE) received the bachelor's degree in electrical engineering from the University of Madras, Chennai, India, in 2002, the master's degree (Hons.) in electrical engineering from Pondicherry University, Puducherry, India, in 2006, and the Ph.D. degree in electrical engineering from the University of Bologna, Bologna, Italy, in 2012. He was an Associate Professor with VIT University from 2012 to 2013. In 2013, he joined the National Institute of Technology, India, as a Faculty Member. In 2014, he was invited as a Visiting Researcher with the Department of Electrical Engineering, Qatar University, Doha, Qatar, funded by the Qatar National Research Foundation (Government of Qatar). He continued his research activities with the Dublin Institute of Technology, Dublin, Ireland, in 2014. Further, he has served as an Associate Professor for the Department of Electrical and Electronics Engineering, University of Johannesburg, Johannesburg, South Africa, from 2016 to 2018. Since 2018, he has been a Faculty Member with the Department of Energy Technology, Aalborg University Esbjerg, Esbjerg, Denmark. He has authored over 300 scientific articles. He was the Best Paper cum Most Excellence Research Paper Award from IET-SEISCON'13, IET-CEAT'16, IEEE-EECSI'19, IEEE-CENCON'19, and five best paper awards from ETAEERE'16 sponsored Lecture Notes in Electrical Engineering, Springer book. He is also a Fellow of the Institution of Engineers, India, the Institution of Electronics and Telecommunication Engineers, India, and the Institution of Engineering and Technology, U.K. He is also an Editor/Associate Editor/Editorial Board of refereed journals, in particular the IEEE Systems Journal, IEEE Transaction on Industry Applications, IEEE Access, *IET Power Electronics*, *IET Electronics Letters*, and Wiley-*International Transactions on Electrical Energy Systems*, the Subject Editorial Board Member—*Energy Sources—Energies Journal*, MDPI, and the Subject Editor of the *IET Renewable Power Generation*, *IET Generation*, *Transmission and Distribution*, and *Facts* journal (Canada).

KAVASKAR SEKAR received the B.E. degree in electrical and electronics engineering from the University of Madras, and the M.E. and Ph.D. degrees in power systems engineering from Anna University, India. He is currently working as an Associate Professor with the Department of Electrical and Electronics Engineering, Panimalar Engineering College. His research interests include artificial intelligence techniques in smart grid, fault detection, and integration of renewable energy sources to grid. He is also a Life Member of the Indian Society for Technical Education.

RAJESWARI RAMACHANDRAN (Member, IEEE) received the bachelor's degree in electrical and electronics engineering and the master's degree in power systems engineering from the Thiagarajar College of Engineering, Madurai, India, in 1995 and 1998, respectively, and the Ph.D. degree from Anna University, Chennai, India, in 2009. She has been an Associate Professor with the Department of Electrical and Electronics Engineering, Government College of Technology, since 2009. Her research interests include power system operation and control (dynamic and stability studies), applying soft computing techniques to power systems.

HASHIM HIZAM (Member, IEEE) received the B.Sc. and M.Sc. degrees in electrical and electronic engineering from Polytechnic University, Brooklyn, NY, USA, in 1993 and 1994, respectively, and the Ph.D. degree from Queens University Belfast, U.K., in 2004. He joined Universiti Putra Malaysia as a Lecturer in 2004, where he is currently an Associate Professor with the Department of Electrical and Electronic Engineering, Faculty of Engineering. In UPM, he has served as the Head for the Electrical and Electronic Engineering Department from 2006 to 2011 and the Deputy Dean for Academic from March 2013 until June 2016. He has published more than 80 journal articles and has successfully supervised several Ph.D. and M.Sc. students. His research interests include power system protection, power system analysis, and renewable energy.

ARANGARAJAN VINAYAGAM (Member, IEEE) received the B.Tech. degree in electrical engineering from RVD University, India, and the Ph.D. degree in PV integrated microgrid power system from Deakin University, Australia. Last, he worked as an Associate Professor with the Electrical and Electronics Engineering Department, Sri Shakthi Institute of Engineering and Technology, Coimbatore, India. He is currently working as an Adjunct Faculty with the New Horizon College of Engineering, Bengaluru, India. He has more than 15 years of industrial experience in the power plant industry and renewable energy technologies. He has more than three years of Academic experience in teaching and research covering the smart grid and microgrid power system, renewable energy technologies, power generation and distribution control, distributed generation sources, and power quality. He has published more than 30 research articles in reputed journals, book chapters, and international conferences. The research interests include developing a smart microgrid power system with integrated solar PV and energy storage facility. Also, expanding research to analyze power quality and electric faults in microgrid and large grid power systems.

MOHAMMAD ZOHRUL ISLAM (Graduate Student Member, IEEE) received the bachelor's degree from the Electrical and Electronic Engineering Department (EEE), International Islamic University Chittagong (IIUC), in 2013. He is currently pursuing the master's degree with the Electrical Power Engineering Department, Universiti Putra Malaysia (UPM). He worked as a Site Engineer under the UREDS Project at Moulvibazar Palli Bidyut Samity from 2013 to 2018. His research interests include artificial intelligence (AI), power systems, and voltage stability. He is also a member of the Institution of Engineers, Bangladesh (IEB), and IEEE Young Professionals Student.